

# Poly(*N*-acylethylenimines) with Pendant Carbazole Derivatives.

## 3. Electrochemical Studies

Bing R. Hsieh and Morton H. Litt\*

Department of Macromolecular Science, Case Western Reserve University,  
Cleveland, Ohio 44106

Kathleen Abbey†

NASA—Lewis Research Center, Cleveland, Ohio 44135. Received September 5, 1985

**ABSTRACT:** The electrochemical properties of carbazole-, 2,7-dimethoxycarbazole-, 3,6-dimethoxycarbazole-, 2,7-dihydroxycarbazole-, and 3,6-dihydroxycarbazole-containing poly(*N*-acylethylenimines), code named p4, p274, p364, p27(OH)4, and p36(OH)4, respectively, and the corresponding model compounds, code named 4CN, 274CN, 364CN, 27(OH)4CN, and 36(OH)4CN, were studied by cyclic voltammetry (CV). The model compounds were studied in 0.1 M TEAP/CH<sub>3</sub>CN. Polymers p4, p274, and p364 were studied as dissolved species in 0.1 M TBAP/CH<sub>2</sub>Cl<sub>2</sub> and as coated materials on a Pt electrode surface in 0.1 M TEAP/CH<sub>3</sub>CN, while p27(OH)4 and p36(OH)4 were studied only as immobilized materials in 0.1 M TEAP/CH<sub>3</sub>CN. The redox potentials of the surface-coated polymers were almost identical with those of their respective model compounds. Polymer p4 underwent cross-linking to form 3,3'-dicarbazyl links and p27(OH)4 showed irreversible CV characteristics and broad peak widths and separations. These agreed well with the oxidation of the respective model compounds 4CN and 27(OH)4CN to form dimer for 4CN and oligomer for 27(OH)4CN. Model compound 274CN showed highly irreversible CV waves, whereas 364CN and 36(OH)4CN showed reversibility. CV waves for the surface-coated p274, p364, and p36(OH)4 showed symmetrical shapes, small peak separations, and peak currents proportional to the scan rate; however, their half-widths were larger than the theoretical value of 90/*n* mV. During continuous CV scans, the electrode coated with p4, p274, or p364 displayed gradually diminishing redox currents and increasing peak separations. In contrast, CV waves for p27(OH)4 and p36(OH)4 remained reproducible after many scans. CV waves for p4, p274, or p364 dissolved in 0.1 M TBAP/CH<sub>2</sub>Cl<sub>2</sub> showed overpotentials after only several scans; green deposits formed on the electrode surface. Anodic currents increased constantly even with the deposits on the electrode, indicating that the oxidized materials may be semiconducting materials. The cathodic current for p4 increased and reached a constant value, while that of p364 or p274 increased initially and disappeared after about 15 cycles. The disappearing cathodic current was attributed to formation of the respective strongly associated perchlorate salts.

## Introduction

Electrochemistry has played a very important role in the field of organic metals. The most prominent example is the discovery of the first group of organic superconductors, namely salts of bi(tetramethyltetraselenafulvalene) cation radical with anions such as PF<sub>6</sub><sup>-</sup>, AsF<sub>6</sub><sup>-</sup>, ClO<sub>4</sub><sup>-</sup>, and so forth.<sup>1</sup> Electrochemical doping is a simple and elegant technique and has been used extensively for the preparation of conducting polymers. For example, polyacetylene has been doped into a p- or n-type conductor by an electrochemical process.<sup>2</sup> Another interesting example is the electrochemically formed polypyrrole films<sup>3</sup> which can be switched reversibly between the insulating (reduced) state and the highly conducting (oxidized) state by applying appropriate potentials.<sup>4</sup>

The versatility of electrochemistry also shows in the current interest in chemically modified electrodes.<sup>5</sup> Of particular importance are electrodes coated with electroactive polymers because of the ease of preparation and the wide range of applications such as electrocatalysis, solar energy conversion, electrochromic bilayer film devices, and so forth. The polymer-modified electrodes can be prepared by (1) physical adsorption (dip<sup>6</sup> or spin coating<sup>7</sup> from polymer solution), (2) surface cross-linking of reactive moieties in a polymer,<sup>8</sup> or (3) surface polymerization of monomers to form polymeric films (such as polypyrrole). The electrooxidation of poly(*N*-vinylcarbazole) (PVK) reported recently by Japanese workers<sup>9</sup> falls into the second category since carbazole cation radicals are highly reactive and undergo dimerization at the 3,6-positions<sup>10</sup> to give cross-linked material containing 3,3'-dicarbazyl. They reported room-temperature conductivities ( $\sigma_{RT}$ ) as high as  $6 \times 10^{-4}$  ( $\Omega$  cm)<sup>-1</sup> for the 50% oxidized material.

Similar results were reported earlier by Block et al., who oxidized PVK with tris(*p*-bromophenyl)ammonium hexachloroantimonate.<sup>11</sup> These findings are stimulating since they demonstrate the possibility of producing good semiconducting pendant group polymers in general and carbazole-containing polymers in particular.

It is well established that the charge, electron, and/or hole migration in PVK-type materials is controlled by a hopping mechanism between traps. PVK happens to provide a matrix for efficient charge migration—more efficient than most non-carbazole-based polymers.<sup>12</sup> Therefore, we decided to work on carbazole derivatives of poly(*N*-acylethylenimines) as the precursors for semiconductors. The reasons for choosing poly(*N*-acylethylenimines) were described in earlier publications.<sup>13</sup>

Although good semiconductivity ( $10^{-2}$   $\Omega^{-1}$ cm<sup>-1</sup>) was predicted for the fully oxidized PVK,<sup>11</sup> this material is undoubtedly highly cross-linked and impossible to process. Thus the application of this material is limited. A direct way of solving this problem is to develop polymers that will not undergo cross-linking when oxidized, in other words to produce redox-reversible carbazole-based polymers by blocking the 3,6-positions on the carbazole ring. For this work we chose oxygenated carbazole derivatives, namely 3,6-dimethoxycarbazole, 2,7-dimethoxycarbazole, 3,6-dihydroxycarbazole, and 2,7-dihydroxycarbazole, as the pendant groups on the poly(*N*-acylethylenimine) backbone. The cation radicals of these carbazoles are stabilized by the electron-donating oxygen functional groups. Furthermore, the oxygen functional groups at the 3,6-positions should directly block the reactive sites, while those at the 2,7-positions should sterically hinder the coupling reaction. In this paper, we report a qualitative electrochemical study of these carbazole polymers.

All polymers and model compounds are designated with the abbreviated symbols shown in Figure 1. For instance, poly[*N*-(9-(2,7-dimethoxycarbazolyl))-5-pentanoyl]-

\* To whom all correspondence should be addressed.

† Present address: Therm-O-Disc, Mansfield, OH 44907.

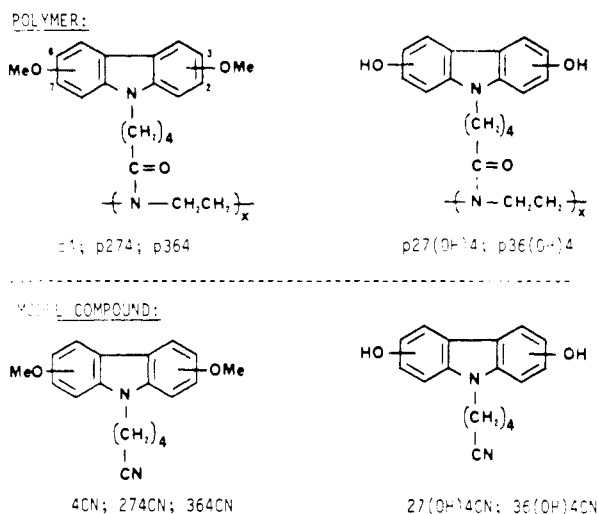


**Figure 1.** Coding for polymers and model compounds.

ethylenimine] and its hydroxy analogue are referred to as p274 and p27(OH)4, respectively, where 2 and 7 indicate the position of the oxygen functional groups, 4 indicates the number of methylene groups attached to the carbazole nitrogen, and (OH) is used when the functional groups are hydroxyl. Only the number of methylene units on the side chain will be used for the unsubstituted carbazole-containing polymers, that is, polymer p4. The model compounds were code named accordingly.

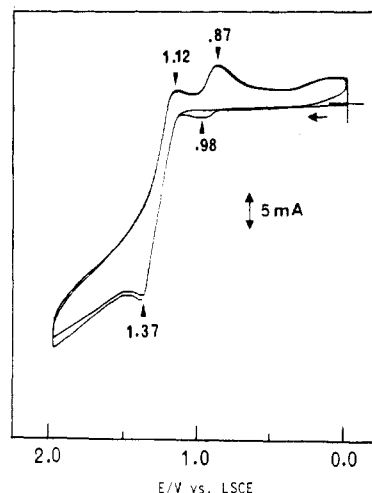
### Experimental Section

**Measurements.** All electrochemical measurements were made with a Princeton Applied Research (PAR) Model 173 potentiostat, Model 175 universal programmer, and Model 179 digital coulometer. Cyclic voltammograms were recorded on a Hewlett-Packard Model 7046A X-Y recorder. All measurements were performed in a single-compartment three-electrode cell. The working electrode was a large cylindrical platinum gauze electrode. The counter electrode was a platinum wire. The reference electrode was a lithium chloride saturated calomel electrode (LSCE) which was isolated from the cell by a salt bridge.

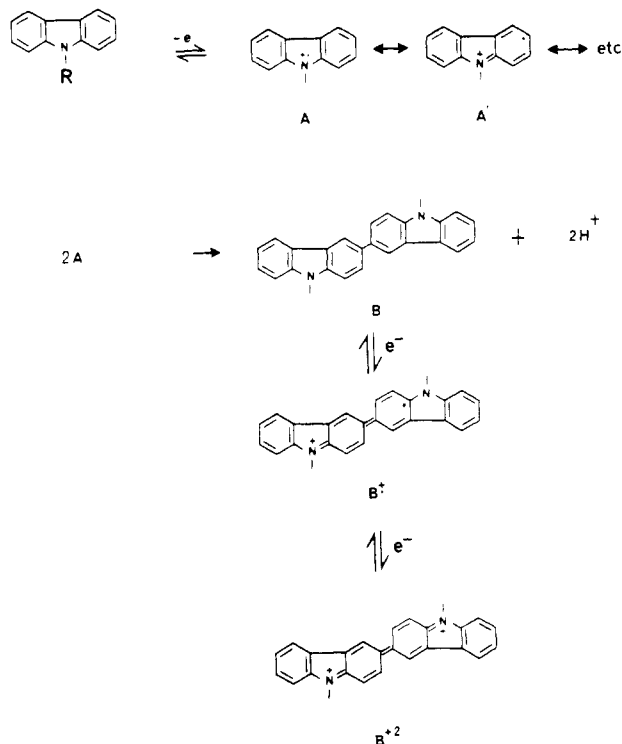
Electrochemical measurements on the model compounds were done in 0.1 M TEAP/CH<sub>3</sub>CN; the model compound concentrations were 2.0 mM. The polymers were studied as 2.0 mM solutions, based on the concentration of carbazole groups, with 0.1 M TBAP in CH<sub>2</sub>Cl<sub>2</sub>. In some cases the polymers were precoated on the electrode according to the following procedure. The Pt working electrode was dipped into and removed quickly from a 0.1% (0.1 g/100 mL) of the polymer solution, p4, p274, or p364 in CH<sub>2</sub>Cl<sub>2</sub> or p27(OH)4 or p36(OH)4 in DMF. The coated electrode was dried in a vacuum oven at 100 °C for 2 h for the hydroxy polymer and 10 min for the methoxy polymer. The cyclic voltammetric study of these coated electrodes was carried out in 0.1 M TEAP/CH<sub>3</sub>CN.

### Results and Discussion

**Electrochemical Study of 4CN and p4.** The cyclic voltammetry (CV) trace of 4CN illustrated in Figure 2 shows oxidation-reduction behavior similar to that reported for N-alkylated carbazoles by Nelson et al.<sup>10</sup> They demonstrated that the oxidation of carbazole as well as N-alkylcarbazoles exhibits the characteristics of a classical ECE mechanism as shown in Figure 3. The cation radical (A<sup>•+</sup>) formed during the initial oxidation peak at 1.37 V dimerizes. The dimer loses two protons to give the 3,3'-dicarbazyl (B), which is oxidized to the cation radical (B<sup>•+</sup>) and then to the dication (B<sup>2+</sup>) at the potential required for the oxidation of the carbazole group. The two one-electron reduction waves shown in Figure 2 are due to the reduction of B<sup>2+</sup> first to B<sup>•+</sup> and then to B. The second anodic scan shows the oxidation of B, which has not yet



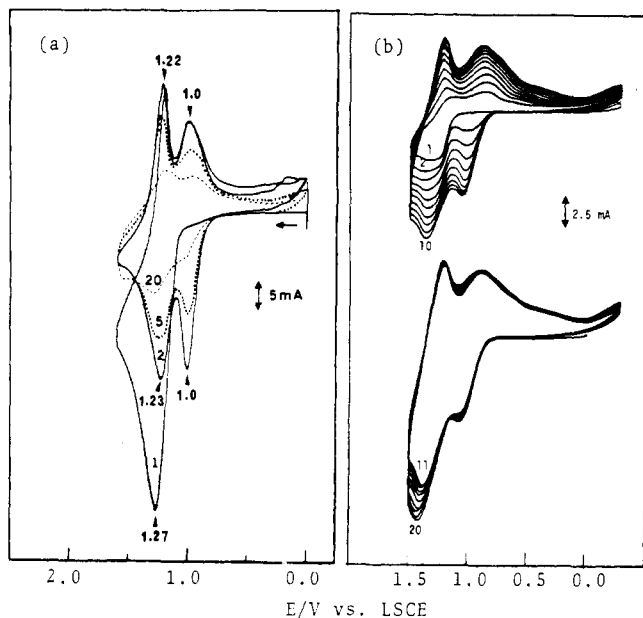
**Figure 2.** Cyclic voltammogram of 4CN at 1 V/s.



**Figure 3.** Oxidation mechanism of N-alkylated carbazole.

diffused away from the electrode surface, to B<sup>•+</sup> at +0.98 V, and then to B<sup>2+</sup> at a higher potential. The small reduction peak at +0.12 V corresponds to the reduction of the protons released in the coupling reaction.

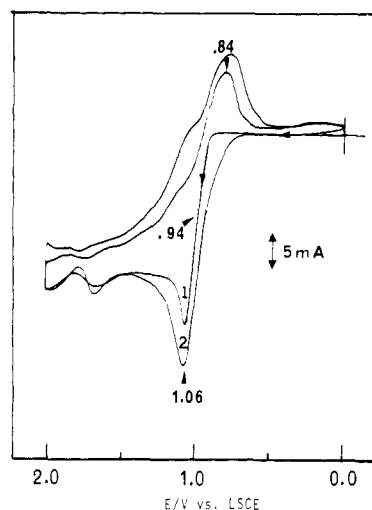
The cyclic voltammogram of p4 deposited on the working electrode from 0.1% polymer/CH<sub>2</sub>Cl<sub>2</sub> is given in Figure 4a, which shows a CV response similar to that seen in the model compound, 4CN. The carbazole groups are oxidized at +1.27 V and couple quickly and irreversibly to form the dicarbazyls, which are responsible for two reduction waves seen in the reverse scan. The subsequent scan shows only the presence of the dimeric species, as indicated by the relatively equal oxidation and reduction currents. This implies that most of the carbazole units have been dimerized in the first sweep. In other words, complete cross-linking occurred after only one scan. In successive scans the peak currents dropped gradually. This may be due to the formation of strongly associated B<sup>2+</sup> and/or B<sup>•+</sup> perchlorate salts whose counterion diffusion from the film is slower than the experimental time scale.



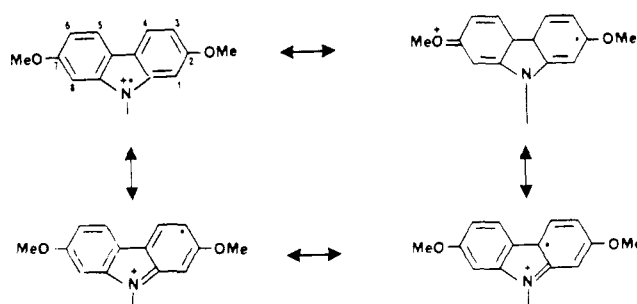
**Figure 4.** (a) Cyclic voltammograms of p4 deposited on an electrode at 200 mV/s. (b) Cyclic voltammograms of p4 dissolved in 0.1 M TBAP/CH<sub>2</sub>Cl<sub>2</sub> at 500 mV/s.

Figure 4b shows electrochemical waves for p4 dissolved in 0.1 M/TBAP/CH<sub>2</sub>Cl<sub>2</sub> with the potential scanned repeatedly between  $-0.3$  and  $+1.5$  V. Formation of dicarbazyl can be seen after the first anodic scan. The gradually increasing redox peak currents in the beginning scans may be due to the growing deposit on the electrode surface. However, reduction peak currents corresponding to the dicarbazyls become constant after the first ten scans. This suggests that formation of the B<sup>2+</sup> and/or B<sup>+</sup> perchlorate salts on the Pt surface is initially slow and becomes faster as salts deposit on the electrode. The peak current corresponding to the oxidation of carbazole groups, on the other hand, continues to increase. The higher current could be because deposition per cycle increases with increasing surface area of the electrode. This salt should be a good semiconductor, as in the case of oxidized PVK, because insulating deposits result in the decrease of the electrochemical current.<sup>15,16</sup> Similar to many organic semiconductors, the semiconductivity in this case may involve electron hopping among the redox centers. As the salts grow, the Pt electrode becomes a semiconductor, which has a much higher resistance than bare Pt, and thus causes the overpotentials seen in the later scans.

**Electrochemical Study of 274CN and p274.** The very complicated cyclic voltammogram of 274CN shown in Figure 5 indicates irreversible reaction. The major oxidation peak of 274CN appears at  $+1.06$  V, which is  $+0.3$  V lower than that for 4CN, followed by a small anodic peak at  $+1.70$  V. The major reduction peak occurs at  $+0.84$  V and is accompanied by many small shoulders. This suggests that there is more than one product. The oxidized 274CN appears as a dark green material strongly adsorbed on the electrode surface. Similar CV response is observed in the second sweep with higher current. Figure 6 depicts the 2,7-dimethoxycarbazole cation radical (C<sup>+</sup>) and its possible resonance forms. This cation radical should be more stable than the carbazole cation radical because of the steric effect and the resonance stabilization of the methoxy groups. It could be oxidized further to the dication at  $+1.7$  V. These ionic species could be very susceptible to nucleophilic attack by trace amounts of water or other basic impurities to give various products. However, coupling reaction of C<sup>+</sup> may be important since the



**Figure 5.** Cyclic voltammograms of 274CN at 500 mV/s.



**Figure 6.** Possible resonance forms for 2,7-dimethoxycarbazole cation radical (C<sup>+</sup>).

controlled-potential electrolysis of 274CN showed an  $n$  value of 2.5. Also the small cathodic peak at  $+0.12$  V suggests the production of protons during the oxidation. No further attempts were made to characterize this system due to its complexity.

Successive CV scans of p274 dissolved in 0.1 M TBAP/CH<sub>2</sub>Cl<sub>2</sub> are shown in Figure 7a. The redox current increases in the first several cycles, but the cathodic current drops to a constant value by the 10th cycle. This may be due to the fast rate of growth of the cation radical and/or dication perchlorate salts, which resist further reduction. The anodic peak current increases continuously, though a small decrease can be seen from the 7th to 11th cycles, indicating that the condensed perchlorate salts may be semiconducting. But the rapid development of the large overvoltage as compared to the case for the carbazole system suggests higher resistivity for the oxidized p274 than the oxidized p4. The peak at  $-0.2$  V may be due to the reduction of protons, which formed in the various coupling reactions, on the polarized electrode.

Results so far all indicate an irreversible process for p274; however, some reversibility was found for the surface-immobilized p274. Theoretically, the CV characteristics of a reversible electrochemical reaction for a surface-confined reactant are (1) symmetrical CV waves, (2) linear proportionality of the peak current with scan rate ( $\nu$ ), (3) small peak potential separation (i.e.,  $\Delta E_p \approx 0$  V), and (4) a value of  $90.6/n$  mV ( $25^\circ\text{C}$ ) for the half-height peak width ( $\Delta E_{1/2}$ ) of an  $n$ -electron process.<sup>17,18</sup> The CV waves of immobilized p274 (Figure 7b) at scan rates of 100, 200 and 500 mV/s have the first three features but show large peak widths in the range 350–500 mV which increase at higher scan rate. The broadening of the surface waves has been reported for many polymers having redox-reversible pendant groups<sup>19</sup> and has been attributed to

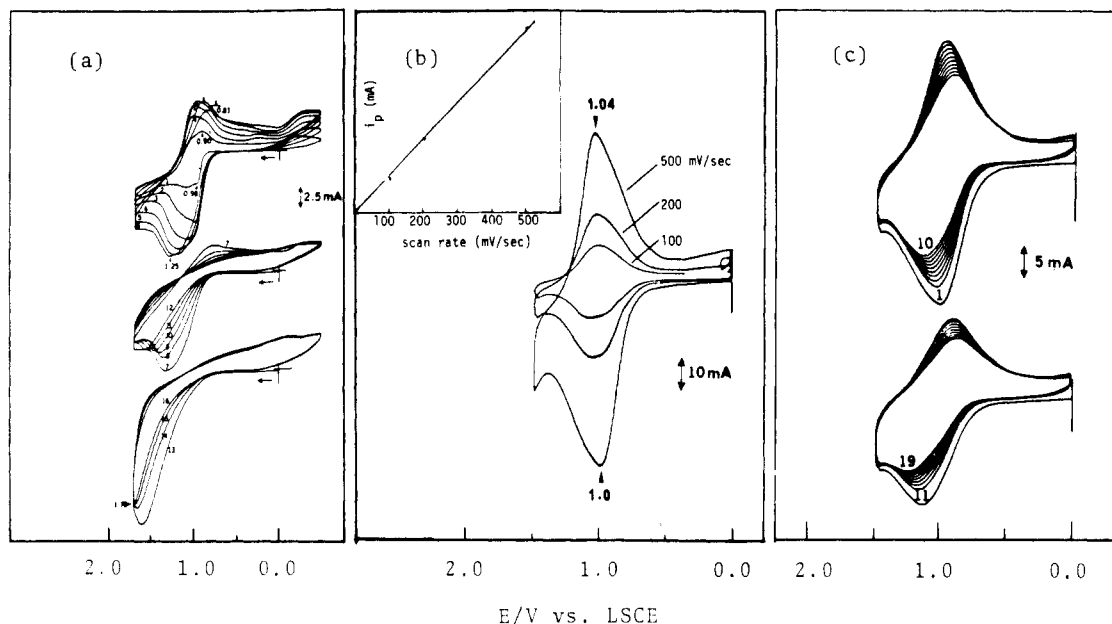


**Figure 7.** (a) Cyclic voltammograms of p274 dissolved in 0.1 M TBAP/CH<sub>2</sub>Cl<sub>2</sub> at 500 mV/s. (b) Cyclic voltammograms of surface-coated p274. The inset shows a plot of anodic peak current against scan rate. (c) Multisweep cyclic voltammograms of surface-coated p274 at 500 mV/s.

various factors, such as a difference in the spatial distribution of the redox centers,<sup>20</sup> a distribution of species with different redox potentials for the electroactive units,<sup>21</sup> and repulsive interactions,<sup>22</sup> depending on the particular system. In the case of p274, repulsive interactions between the oxidized species should be important since C<sup>+</sup> is relatively stable and thus may have a long lifetime. The broad peaks of p274 could also be due to the formation of a small amount of dimeric groups and/or so-called mixed-valence aggregates such as (C)<sub>2</sub><sup>+</sup>, since the model compound 274CN shows irreversible behavior. In some tetrathiafulvalene (TTF)-containing polymers, mixed-valence species (TTF)<sub>2</sub><sup>+</sup> were reported to be responsible for the broad redox waves. In the successive scans of immobilized p274 (Figure 7c), the redox peak currents drop constantly and the anodic and cathodic peaks gradually drift apart. This may be due to gradual formation of the strongly associated perchlorate salts from the electrode surface outward. As soon as the salts in the inner layers form, the electrode becomes passivated, resulting in overpotentials in the following scans. This again suggests that oxidized p274 has a high resistance compared to the oxidized carbazole polymer, because there was no overpotential found in the oxidized thin carbazole polymer film (Figure 4a). The quasireversible CV waves of immobilized p274 are very different from the irreversible behaviors of 274CN and p274 in solution. This is interesting and understandable since the electroactive groups on the coated surface are less mobile and the possibility of reacting with each other is thus reduced.

**Electrochemical Study of 27(OH)4CN and p27(OH)4.** The cyclic voltammogram of 27(OH)4CN, as depicted in Figure 8a, is somewhat similar to that of 274CN in shape and very complicated. There is an anodic peak at 1.03 V in the forward scan, followed by a major cathodic peak at 0.8 V in the reverse scan. The number of electrons transferred was 2.5. During the electrolysis, a gray precipitate was produced quickly. The broad peaks shown by the material's NMR spectrum (Figure 9a) suggests that it may be an oligomer. The peaks shown in Figure 9a are labeled, from the downfield peaks upward, as peaks a–g and their approximate intensity ratios are 1:1:1:2:1:2:3, respectively. (For comparison, the NMR spectrum of

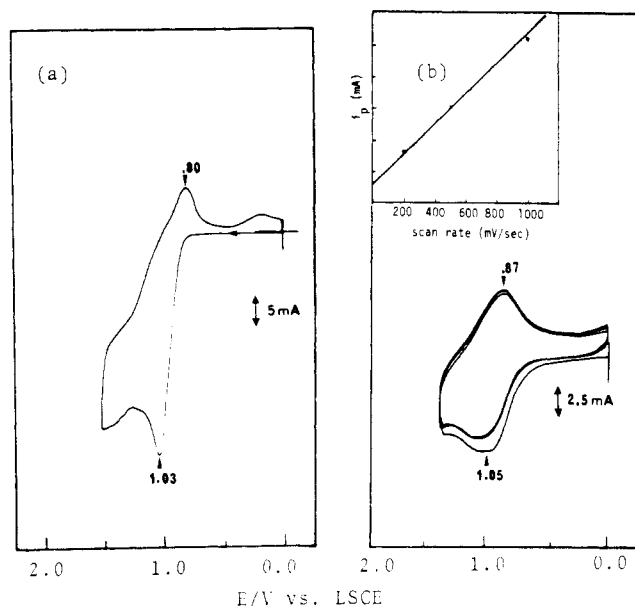


**Figure 8.** (a) Cyclic voltammogram of 27(OH)4CN at 500 mV/s. (b) Cyclic voltammograms of immobilized p27(OH)4 at 500 mV/s. Inset shows a plot of anodic peak current vs. scan rate.

27(OH)4CN is given in Figure 9b.) These spectra are not enough for a complete identification of the structure; nevertheless, they provide some important information. First, note the approximately equal intensity of the aromatic proton peaks, peaks a and b. If there is no reaction of the carbazole ring, the intensity ratio for peaks a and b should be 1:2 as is that for 27(OH)4CN. Therefore, a coupling reaction may be taking place via 3,6 ring sites. It is also likely that the oxidized 27(OH)4CN is associated with the tetraethylammonium cation (Et<sub>4</sub>N<sup>+</sup>), since there are peaks, peaks d and g, due to the protons of the ethyl groups on a quaternary nitrogen. The intensity ratios show there are two oxidized 27(OH)4CN units associated with one Et<sub>4</sub>N<sup>+</sup>. Based on these analyses, a postulated structure for this product is given in Figure 9a, where the protons are labeled with the same letters as the corresponding peaks, assuming that the coupling reaction is via the 3,6-positions. The absence of an isolated peak for the phenoxy

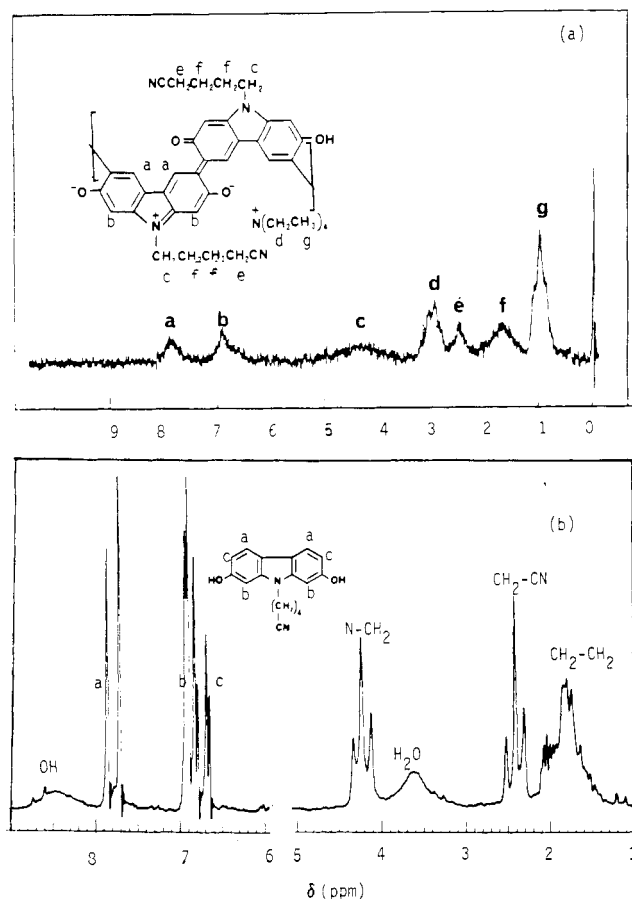


**Figure 9.** (a) NMR spectrum of the oxidized 27(OH)4CN in  $\text{Me}_2\text{SO}-d_6$ . (b) NMR spectrum of 27(OH)4CN in acetone- $d_6$ .

proton could be rationalized by the possibility that it is overlapped by the peak due to the protons on the methylene group attached to the carbazole nitrogen.

The cyclic voltammogram for the surface-deposited p27(OH)4 in 0.1 M TEAP/ $\text{CH}_3\text{CN}$  at a scan rate of 500 mV/s is given in Figure 8b. As in previous examples, the redox peak potentials for p27(OH)4 are essentially the same as those of its model compound 27(OH)4CN. The redox waves are reproducible even after many cycles and the anodic peak current is proportional to the scan rate. But the CV waves are far from symmetrical and very broad, indicative of irreversible behavior. Based on the results for the oxidation of 27(OH)4CN, it is reasonable to assume that the very broad anodic waves are due primarily to the coupling reactions of the pendant groups. However, the reproducible CV waves suggest oxidized p27(OH)4 could be a reversible material.

Phenoxy-type systems, such as aminophenols, phenols, hydroquinones and so forth, generally show very complicated electrochemical reactions. For example, redox reaction of *p*-benzoquinone/hydroquinone, which involves an apparent direct exchange of two electrons and two protons, is not yet fully understood and has been the object of some recent investigations.<sup>23</sup> The phenoxy-type systems are generally studied in buffered aqueous solution because the reaction paths are highly pH dependent. Moieties such as 2,7-dihydroxycarbazole could be regarded as a phenol, an aminophenol, or a heterocyclic hydroquinone; therefore its electrochemical reactions should probably be studied in a buffered solution for a better understanding. However, no further effort was made to study this system, because the next two systems showed reversibility.

**Electrochemical Study of 364CN and p364.** As expected, 364CN showed reversible CV characteristics. The

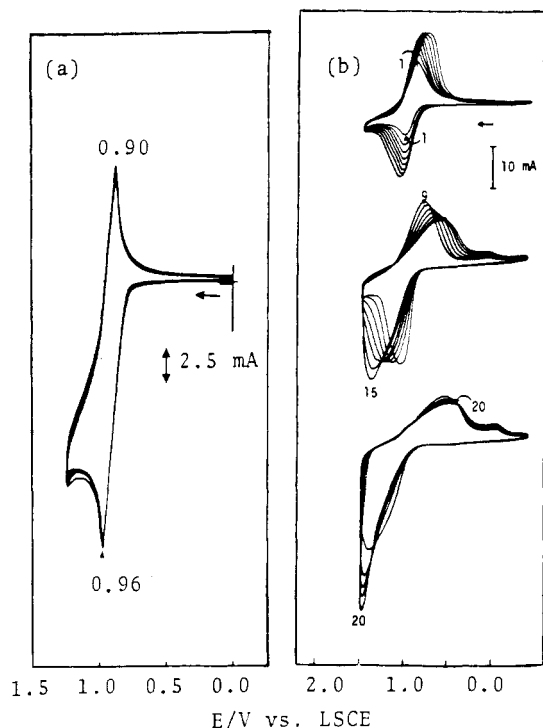


**Figure 10.** (a) Cyclic voltammograms of 364CN at 500 mV/s. (b) Multisweep CV waves of p364 dissolved in 0.1 M TBA/ $\text{CH}_2\text{Cl}_2$ .

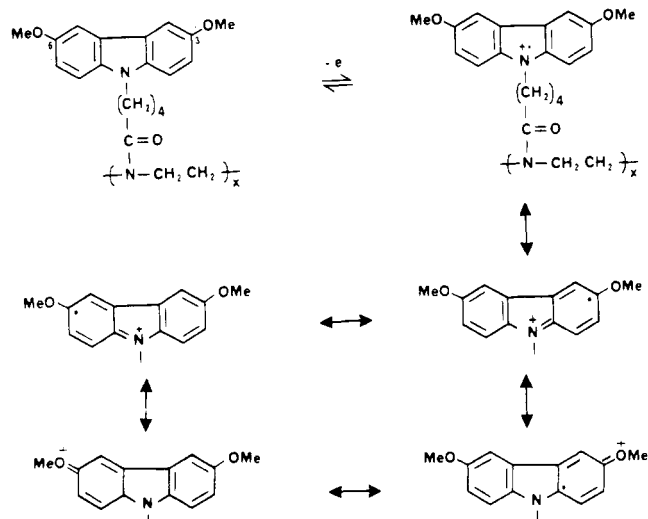


**Figure 11.** Important resonance forms for 3,6-dimethoxycarbazole cation radical ( $\text{D}^{+\bullet}$ ).

CV waves of 364CN (Figure 10a) are highly reproducible and show an anodic peak at +0.96 V and a cathodic peak at +0.90 V. The peak separation of 60 mV fits nicely with the theoretical value for a one-electron-transfer reaction. Similar to earlier cases the oxidized solution of 364CN was light green, which disappeared in the cathodic scan. Unlike those previous examples, however, there was no deposit on the electrode surface during the CV cycles and controlled-potential electrolysis. This reversible behavior can be attributed to the stable cation radical  $\text{D}^{+\bullet}$ , which has many resonance forms as depicted in Figure 11 and very low charge density at the 1 and 8 ring sites.<sup>10</sup>

The continuous CV scans of p364 dissolved in 0.1 M TBAP/ $\text{CH}_2\text{Cl}_2$  are illustrated in Figure 10b. The cathodic peak current increases to a maximum value, which then drops gradually in successive scans as the cathodic peak potential moves toward more negative values. This may be a result of the formation of the perchlorate salt ( $\text{D}^{+\bullet}\text{ClO}_4^-$ ), which polarizes the electrode and causes overvol-

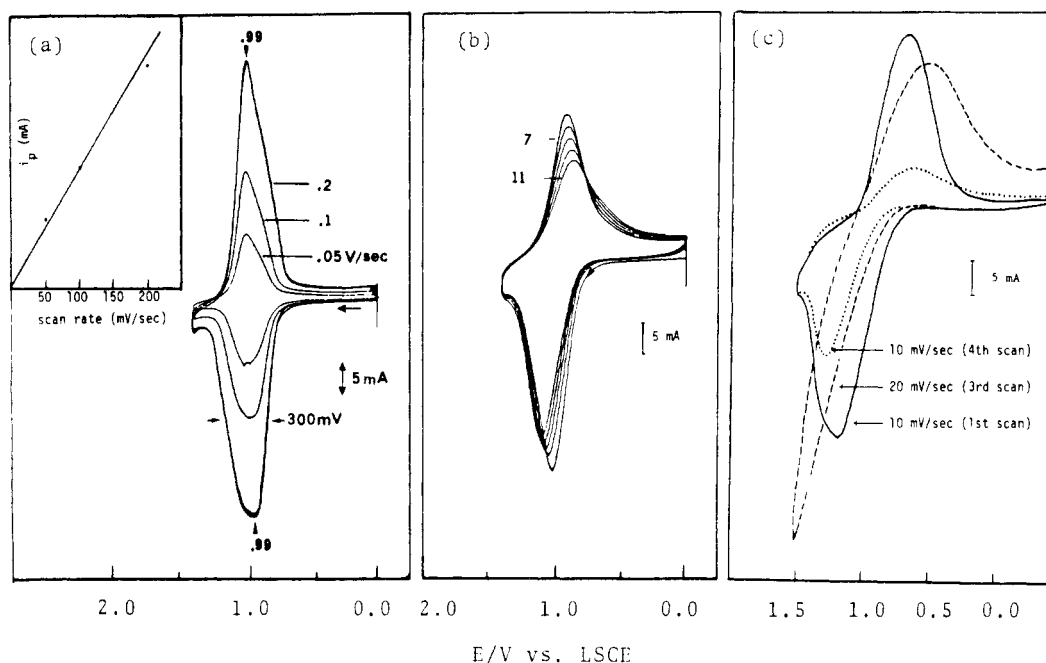


**Figure 12.** (a) Cyclic voltammograms of surface-coated p364 at different scan rates. Inset shows a plot of anodic peak current vs. scan rate. (b) Multisweep CV waves (7th to 11th cycles) for surface-coated p364 at 200 mV/s. (c) CV waves for a thicker film of p364 deposited on an electrode surface.

tages in both cathodic and anodic waves. The continuous decrease in the cathodic current indicated that the rate of  $D^+ \cdot ClO_4^-$  formation is increasing. The anodic currents though remain relatively constant from the 10th to 13th cycles but increase quickly from the 14th cycle on. This increase in anodic current could be due to the increasing electrode surface area, due to the growing  $D^+ \cdot ClO_4^-$ , and indicates that oxidation is still going strong on the passivated surface. A small peak starts to appear in the 9th cycle at ca. 0 V and moves gradually to more negative values. These peaks could be due to the reduction of protons, which were produced from a side reaction between  $D^+$  and water or other impurities.<sup>10a</sup>

The cyclic voltammograms of surface-coated p364 (Figure 12a) show some reversibility. First, peak-to-peak separations are essentially zero at scan rates of 50, 100, and 200 mV/s, as expected for a reversible surface-confined redox reaction. In addition, the anodic peak current is directly proportional to the scan rate. One feature of the CV waves is not in accord with the criteria for an immobilized reversible reactant. According to theory the width at half-height of either the cathodic or anodic wave should be about 90 mV; however, peak half-widths in this case are in the range 200–350 mV and increase with increasing scan rate. The broad anodic peaks in the initial scans could be a result of repulsive interaction and/or formation of mixed-valence species. Further, the cathodic waves are initially narrower than the anodic waves ( $\Delta E_{1/2} = 200$  and 300–500 mV, respectively). After several scans (Figure 12b) the latter begin to decrease in height and become much broader. It is possible that the oxidized centers near the surface form  $D^+ \cdot ClO_4^-$  first, which then cause overpotentials in subsequent scans. Condensation of the cation radical salt also reduces the repulsive force and results in sharper anodic waves ( $\Delta E_{1/2} = 200$  mV).

Figure 12c shows the CV behavior at slow scan rates of surface-coated p364, cast from 5% p364/ $CH_2Cl_2$  in 0.1% TBAP/ $CH_3CN$ . The increase in  $\Delta E_{1/2}$  and  $\Delta E_p$  is due to higher resistance which may in turn be due to very slow counterion diffusion rate through thicker films, as reported for thick films (ca. 400 nm) of TTF-containing polymers.<sup>7</sup>

The third cycle at higher scan rate, 20 mV/s, shows even higher  $\Delta E_p$ . Formation of the cation radical salt in this case is reflected by the rapid drop of the cathodic current.

**Electrochemical Study of 36(OH)4CN and p36-(OH)4.** Cyclic voltammograms of 36(OH)4CN dissolved in 0.1 M TEAP/ $CH_3CN$  are shown in Figure 13a. These CV waves are very poorly resolved at scan rates lower than 500 mV/s, indicating irreversibility. This may be because of many reaction intermediates, perhaps due to the involvement of protons in the reaction, similar to the *p*-benzoquinone/hydroquinone couple. This couple is a  $2e^-$ ,  $2H^+$  process, which has nine possible species as represented in the nine-membered square scheme shown in Figure 14,<sup>23a</sup> and shows irreversible behavior in aprotic solvents.<sup>23b</sup> Despite the apparent irreversibility of 36(OH)4CN, its anodic current shows Nernstian characteristics; that is, the peak current is proportional to the square root of the scan rate (Figure 13a, inset). Based on a possible  $2e^-$ ,  $2H^+$  process, a simplified reaction scheme for 36(OH)4CN is given in Figure 15.

CV waves for surface-coated p36(OH)4 in 0.1 M TEAP/ $CH_3CN$  are given in Figure 13b. Except for the first cycle, all waves show reproducibility, symmetry, and no peak separation. The overpotential in the first cycle may be due to the high resistance in a newly coated electrode, which will absorb electrolyte after the first cycle and become conductive. It is also possible that the starting p36(OH)4 is more difficult to oxidize as compared with the deprotonated intermediates shown in Figure 15. In addition, the peak current is proportional to the scan rate. However, the half-height peak widths, about 350 mV for the anodic wave and 225 mV for the cathodic wave, are higher than the theoretical value, 45 mV for a  $2e^-$  reaction. These large peak widths could be due to repulsive interaction etc. factors discussed earlier. But the main factor in this system could be formation of many intermediates during oxidation. It is interesting to note that CV waves for p36(OH)4 are closer to ideal than those of 36(OH)4CN.

#### Overall Considerations

The electrochemical properties of the model compounds are summarized in Table I. Among these compounds,

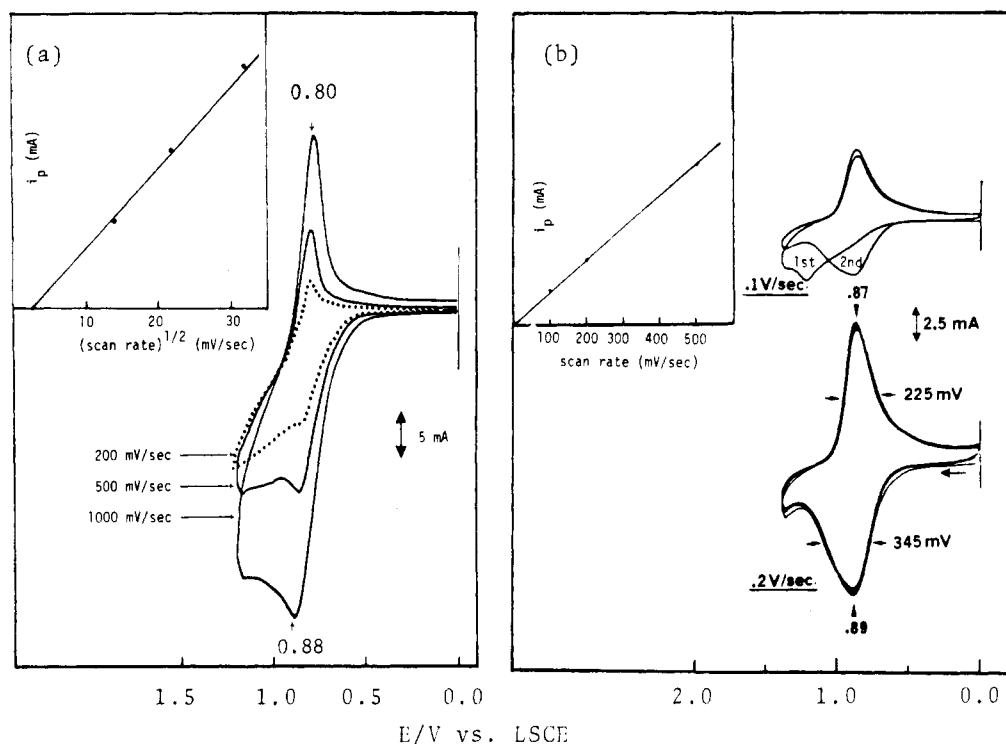


**Figure 13.** (a) Cyclic voltammograms of 36(OH)4CN at different scan rates. Inset shows a plot of anodic peak current vs. square root of scan rate. (b) Cyclic voltammograms of surface-coated p36(OH)4. Inset shows a plot of anodic peak current vs. scan rate.

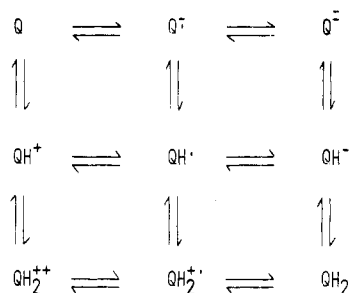


**Figure 14.** Reaction scheme of *p*-benzoquinone/hydroquinone couple.

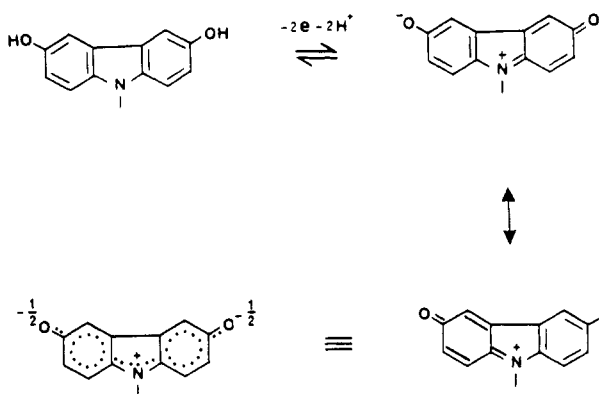


**Figure 15.** Simplified reaction scheme of p36(OH)4 or 36(OH)4CN.

4CN, 274CN, and 27(OH)4CN are clearly irreversible while 364CN and 36(OH)4CN show some reversibility. The  $\Delta E_p$  for 364CN is 0.06 V, which corresponds to a  $1e^-$  reaction, if reversible. However, an  $n$  value of 2.3 was found when 364CN was electrolyzed until almost zero current and an  $n$  value of 1.5 was found when the electrolysis was stopped at the onset of a steady-state current. The  $n$  value of 1.5 instead of 1.0 could be due to impurities in the system, since a similar molecule, namely *N*-ethyl-3,6-dimethoxy-

**Table I**  
Electrochemical Data for the Model Compounds

compd	$(E_p)_a$ , V	$(E_p)_c$ , V	$\Delta E_p$ , V <sup>a</sup>	$n$ value <sup>b</sup>	remarks
4CN	1.37			3.1	green deposit
274CN	1.06	0.82	0.24	2.5	green deposit
364CN	0.96	0.90	0.06	1.5	green solution at $(E_p)_a$
27(OH)-4CN	1.03	0.80	0.23	2.5	gray deposit
36(OH)-4CN	0.88	0.84	0.04	2.0 <sup>c</sup>	green solution at $(E_p)_a$

<sup>a</sup>  $\Delta E_p = (E_p)_a - (E_p)_c$ . <sup>b</sup> The  $n$  value was determined by using controlled-potential electrolysis of  $1.0 \times 10^{-3}$  M solutions of carbazoles in 0.1 M TEAP/CH<sub>3</sub> at 100 mV higher than the respective  $(E_p)_a$ . Low steady-state currents, which were different for each compound, were observed at these  $n$  values. <sup>c</sup> Steady-state current dropped to zero.

**Table II**  
Electrochemical Data for the Surface-Confined Polymers<sup>a</sup>

polymer	$(E_p)_a$ , V	$(E_p)_c$ , V	$\Delta E_p$ , V <sup>b</sup>	$\Delta E_{1/2}$ , mV	remarks
p4 <sup>c</sup>	1.27				cross-linked
p274 <sup>c</sup>	1.02	0.98	0.04	450-550	quasi-reversible
p364 <sup>c</sup>	0.98	0.95	0.03	300	reversible
p27(OH)4	1.05	0.87	0.18	large	irreversible
p36(OH)4	0.89	0.87	0.02	225-345	reversible

<sup>a</sup> Data based on electrode dip-coated from 0.1% polymer/CH<sub>2</sub>Cl<sub>2</sub>. <sup>b</sup>  $\Delta E_p = (E_p)_a - (E_p)_c$ . <sup>c</sup> Data based on the initial scan.

carbazole, had an  $n$  value of 1.01 at the onset of a steady-state current as reported by Nelson et al.<sup>10</sup> Compound 36(OH)4CN shows the expected  $n$  value of 2.0,  $\Delta E_p$  of 0.04 V, and irreversible CV waves at the scan rates investigated.

The cyclic voltammetric properties of the surface-coated polymers are listed in Table II. The most noteworthy feature of Table II, as compared with Table I, is the almost identical redox potentials of the polymers and those of the respective model compounds. These results suggest the

absence of substantial electronic interactions between the electroactive centers within the polymers. Similar observations have been reported for polymers such as poly(vinylferrocene),<sup>24</sup> poly(nitrostyrene),<sup>25</sup> and some TTF-containing polymers<sup>7</sup> coated on electrode surface. This similarity demonstrated that the predictability of redox potentials, which was first found for monolayers of electroactive reagents covalently bound at the electrode surface, also holds for surface-coated thin polymer films. Such predictable properties would enable one to design new materials with desired electrochemical properties.

Although the peak separations for polymers p274, p364, and p36(OH)4 are relatively small, their half-height peak widths are considerably larger than the theoretical value of  $90/n$  V for an  $n$ -electron reversible reaction. This indicates that electronic interactions exist, although not substantial enough to cause different redox potentials between the polymers and the corresponding model compounds. As already mentioned in the discussion, broadening of the surface waves is frequently seen in various polymers for various reasons. The broad waves for p274 and p364 could be due to repulsive interactions based on the following rationale. At early stages of the oxidation, oxidized groups will be surrounded by neutral groups, which can donate partial charge to them. The potentials required to oxidize these neutral groups surrounding the oxidized groups would be higher than those needed for oxidizing free groups. Therefore, electroactive groups with different oxidation potentials are created and lead to broadening of the anodic peaks. Similarly, broad cathodic peaks result.

During continuous CV scans, the electrode coated with polymer p4, p274, or p364 showed gradually decreasing redox currents and increasing overvoltages, and hence peak separations. On the other hand, CV waves for electrodes coated with p27(OH)4 or p36(OH)4 remained unchanged after many cycles. These results may be due to formation of strongly associated cation radical and/or dication perchlorate salts in the former case. In the latter case, the oxidized hydroxycarbazoles are neutral and do not form salts with electrolyte ions.

CV waves for p4, p274, or p364 dissolved in 0.1 M TBAP/ $\text{CH}_2\text{Cl}_2$  showed overpotentials quickly after several scans, along with green deposits on the electrode surface. The anodic current increased constantly in spite of the overpotentials, indicating that oxidation was still going strong on the deposited electrode. This increase in anodic current indicates that the green deposits may be conducting materials, since insulating deposits result in the drop of anodic current.<sup>16</sup> As the CV scans continued, the cathodic peaks for p274 and p364 shifted to more negative potentials, while the cathodic peak potential for p4 remained unchanged. This may imply that oxidized p4 is a better semiconductor than oxidized p274 and p364. The semiconduction mechanism probably involves electron hopping among the redox centers. The cathodic peak current of p4 increased gradually to a constant while the cathodic peak currents of p274 and p364 increased to a maximum value and then dropped to small values after about 20 cycles. Formation of strongly associated cation radical salts may occur to a larger extent in the oxidation of p274 and p364 than that of p4, resulting in the disappearing cathodic current for the former two. This is understandable, since oxidation of p4 gives cross-linked material, which should have an irregular structure and thus prevent the growth of a regular packed ion radical salt. The regular structure of the poly(*N*-acylethylenimine) backbone may favor formation of crystalline (or highly

associated) ion radical salts in the oxidation of p274 and p364.

The solution CV behaviors of p4, p274, and p364 observed in our study are very similar to that found in the electrochemical growth of conducting  $(\text{FA})_2^+\cdot\text{X}^-$  salts, where FA = fluoranthene and  $\text{X}^- = \text{PF}_6^-$ ,  $\text{SbF}_6^-$ ,  $\text{AsF}_6^-$ ,  $\text{ClO}_4^-$ , and  $\text{BF}_4^-$ , reported by Enkelmann et al.<sup>27</sup> The multisweep CV of FA in 0.1 M  $\text{TBA}^+\text{X}^-/\text{CH}_2\text{Cl}_2$  had the following features: (1) an increasing anodic current, which was attributed to the growing coverage of conducting  $(\text{FA})_2\text{X}$  on the electrode; (2) a diminishing cathodic current, because the crystallized  $(\text{FA})_2\text{X}$  did not reduce easily; (3) overpotentials, which were attributed to the larger resistance of  $(\text{FA})_2\text{X}$  as compared to the bare Pt electrode. This larger resistance resulted in a higher overvoltage necessary to continue the growth process. This finding suggests the possibility that the oxidized polymer salts could be crystalline, especially in the cases of p274 and p364, because  $(\text{FA})_2\text{X}$  can be grown as single crystals or polycrystalline materials depending on the potential setting. Therefore, future work will focus on the conductivity as well as the crystallinity and morphology of the oxidized polymer salts.

**Acknowledgment.** This work was supported by NASA—Lewis Research Center, Cleveland, OH, under Grant No. NAG3-234. Most of the electrochemical studies were done at NASA—Lewis Research Center. We thank the Center for the use of its facilities.

## References and Notes

- (a) Jerome, D.; Mazand, A.; Ribault, M.; Bechgaard, K. *J. Phys. Lett.* **1980**, *41*, L95. (b) Bechgaard, K.; Jacobson, C. S.; Mortensen, K.; Pedersen, H. J.; Thorup, N. *Solid State Commun.* **1980**, *33*, 1119.
- Chiang, C. K.; Blubaugh, E. A.; Yap, W. T. *Polymer* **1984**, *25*, 1112 and references therein.
- (a) Diaz, A. F.; Kanazawa, K. K.; Gardini, G. P. *J. Chem. Soc., Chem. Commun.* **1979**, 635. (b) Diaz, A. F.; Kanazawa, K. K.; In "Extended Linear Chain Compounds"; Miller, J. S., Ed.; Plenum Press: New York, 1982; p 417 and references therein.
- (a) Bull, R. A.; Fan, F. F.; Bard, A. J. *J. Electrochem. Soc.* **1982**, *129*, 1009. (b) Diaz, A. F.; Castillo, J.; Kanazawa, K. K.; Logan, J. A. *J. Electroanal. Chem.* **1982**, *133*, 233.
- Faulkner, L. R. *Chem. Eng. News* **1984**, 62(9), 28 and references therein.
- (a) Degrand, C.; Miller, L. L. *J. Electroanal. Chem.* **1981**, *117*, 267. (b) Funt, B. L.; Hoang, P. M. *J. Electroanal. Chem.* **1983**, *154*, 229. (c) Degrand, C.; Miller, L. L. *J. Am. Chem. Soc.* **1980**, *102*, 5728. (d) Miller, L. L.; Kerr, J. B. *J. Am. Chem. Soc.* **1979**, *101*, 263.
- (a) Kaufman, F. B.; Schroeder, A. H.; Engler, E. M.; Kramer, S. R.; Chambers, J. Q. *J. Am. Chem. Soc.* **1980**, *102*, 483. (b) Schroeder, A. H.; Kaufman, F. B.; Patel, V.; Engler, E. M. *J. Electroanal. Chem.* **1980**, *113*, 192.
- (a) Kaufman, F. B.; Schroeder, A. H.; Patel, V. V.; Nichols, K. H. *J. Electroanal. Chem.* **1982**, *132*, 151. (b) Kaufman, F. B.; Engler, E. M. *J. Am. Chem. Soc.* **1979**, *101*, 547.
- (a) Kanega, H.; Shirota, Y.; Mikawa, H. *J. Chem. Soc., Chem. Commun.* **1984**, 158. (b) Davis, F. J.; Block, H.; Compton, R. G. *J. Chem. Soc., Chem. Commun.* **1984**, 890.
- (a) Ambrose, J. F.; Carpenter, L. L.; Nelson, R. F. *J. Electrochem. Soc.* **1975**, *122*, 876. (b) Ambrose, J. F.; Nelson, R. F. *J. Electrochem. Soc.* **1968**, *115*, 1159.
- (a) Block, H.; Cowd, M. A.; Walker, S. M. *Polymer* **1977**, *18*, 781. (b) Block, H.; Bowker, S. M.; Walker, S. M. *Polymer* **1978**, *19*, 531.
- (a) Mort, J. *Adv. Phys.* **1980**, *29*, 367. (b) Penwell, R. C.; Ganguly, B. N.; Smith, T. W. *J. Polym. Sci., Macromol. Rev.* **1978**, *13*, 63. (c) Biswas, M.; Das, S. K. *Polymer*, **1982**, *23*, 1713.
- (a) Litt, M. H.; Rahl, F.; Roldan, L. G. *J. Polym. Sci., Part A-2* **1969**, *7*, 463. (b) Litt, M. H.; Summers, H. W. *J. Polym. Sci., Part A-2* **1973**, *11*, 1339.
- Sawyer, D. T.; Roberts, J. L., Jr. "Experimental Electrochemistry for Chemists"; Wiley: New York, 1974; p 212.
- Bargon, J.; Mohmand, S.; Waltman, R. J. *IBM J. Res. Devel.* **1983**, *27*, 330.



- (16) Lund, H. *Acta Chem. Scand.* **1957**, *11*, 1325.  
 (17) Bard, A. J.; Faulkner, L. R. "Electrochemical Methods"; Wiley: New York, 1980; Chapter 12.  
 (18) (a) Laviron, E. *J. Electroanal. Chem.* **1974**, *52*, 355. (b) Laviron, E. *J. Electroanal. Chem.* **1974**, *52*, 395. (c) Laviron, E. *J. Electroanal. Chem.* **1975**, *63*, 245.  
 (19) Bard, A. J.; Pearce, P. J. *J. Electroanal. Chem.* **1980**, *114*, 89 and references therein.  
 (20) Itaya, K.; Bard, A. J. *Anal. Chem.* **1978**, *50*, 1487.  
 (21) Wrighton, M. S.; Pallazzotto, M. C.; Bocarsly, A. B.; Bolts, J. M.; Fischer, A. B.; Nadjo, L. *J. Am. Chem. Soc.* **1978**, *100*, 7264.  
 (22) (a) Lenhard, J. R.; Murray, R. W. *J. Am. Chem. Soc.* **1978**, *100*, 7870. (b) Kuo, K.; Moses, P. R.; Lenhard, J. R.; Green, D. C.; Murray, R. W. *Anal. Chem.* **1979**, *51*, 745. (c) Smith, D. F.; William, K.; Kuo, K.; Murry, R. W. *J. Electroanal. Chem.* **1979**, *95*, 217.  
 (23) (a) Lavir, E. *J. Electroanal. Chem.* **1984**, *164*, 213 and references therein. (b) Eggins, B. R.; Chambers, J. Q. *J. Chem. Soc., Chem. Commun.* **1969**, 232.  
 (24) Bard, A. J.; Merz, A. J. *Am. Chem. Soc.* **1978**, *100*, 3222.  
 (25) (a) Van Demark, M. R.; Miller, L. L. *J. Am. Chem. Soc.* **1978**, *100*, 3223. (b) Miller, L. L.; Van Demark, M. R. *J. Electroanal. Chem.* **1978**, *88*, 437.  
 (26) Lenhard, J. R.; Rocklin, R.; Abruna, H.; William, K.; Kuo, K.; Nowak, R.; Murrar, R. W. *J. Am. Chem. Soc.* **1978**, *100*, 5213.  
 (27) Enkelmann, V.; Morra, B. S.; Krohnke, Ch.; Wegner, G.; Heinze, J. *J. Chem. Phys.* **1982**, *66*, 303.

## Regioselectively Modified Stereoregular Polysaccharides. 8. Synthesis and Functions of Partially 3-O-Octadecylated (1→6)- $\alpha$ -D-Glucopyranans

Kazukiyo Kobayashi,\* Hiroshi Sumitomo, and Haruo Ichikawa

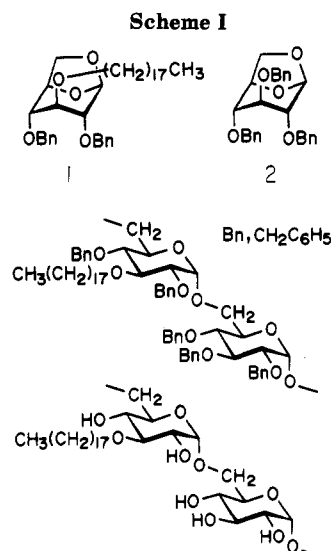
Faculty of Agriculture, Nagoya University, Chikusa, Nagoya 464, Japan.

Received August 6, 1985

**ABSTRACT:** Ring-opening copolymerization between 1,6-anhydro-2,4-di-*O*-benzyl-3-*O*-octadecyl- $\beta$ -D-glucopyranose (1) and 1,6-anhydro-2,3,4-tri-*O*-benzyl- $\beta$ -D-glucopyranose (2) was carried out in the presence of  $\text{PF}_5$  initiator at  $-60^\circ\text{C}$ . The reactivity of monomer 1 was high, and stereoregular homo- and copolymers of high molecular weight were obtained. Debenzylation of the copolymers with sodium metal in liquid ammonia produced (1→6)- $\alpha$ -D-glucopyranans having a 3-*O*-octadecyl group, the degree of substitution (DS) of which was up to 0.22. The following findings on properties of the polysaccharides were obtained. (1) The polysaccharides were hydrolyzed by a dextranase. (2) An organic solute magnesium 1-anilino-8-naphthalenesulfonate was bound to a hydrophobic region of the polysaccharides in water, indicating that the polysaccharides formed a micellar conformation. (3) Flexible membranes of the polysaccharides (DS 0.07–0.22) could be cast from dimethyl sulfoxide solutions. (4) The polysaccharides (DS 0.01–0.05) could be incorporated into liposomes by anchoring the long hydrocarbon chains into the lipid layer of the liposomes, and the resulting polysaccharide-coated liposomes could be isolated. The anchoring effect of the hydrocarbons and the conformation of the polysaccharides on the liposomes are discussed.

Well-defined polysaccharides having both membrane-forming abilities and recognition functions are of interest as a polymeric model of glycolipids. Glycolipids occurring in cell membranes are composed of oligosaccharides and lipids and play an important role in cellular recognition.<sup>1</sup> Glycolipids and their analogues were synthesized and incorporated into cell membranes, and the resulting artificial assemblies proved useful for investigations of various cellular phenomena.<sup>2,3</sup> Incorporation of synthetic glycolipids into a cell-membrane model, liposome, is also extensively investigated, especially for the application of a drug delivery system that employs carbohydrate moieties as recognition markers to target specific organs.<sup>4–8</sup> For this purpose, a strengthening of the liposomal structure is required, and synthesis of polymerized glycolipid models<sup>9–11</sup> and surface coating of liposomes with polysaccharides<sup>12–15</sup> have been attempted. Polysaccharide-coated liposomes were reported by Sunamoto:<sup>14,15</sup> naturally occurring polysaccharides such as dextrans, pullulans, and amylopectins were modified with long-chain fatty acids and assembled into liposomes. It was found that these polysaccharide-coated liposomes were effective for stabilization of liposomes and also for targeting.

In this paper, 3-*O*-octadecylated (1→6)- $\alpha$ -D-glucopyranans capable of forming polysaccharide-coated liposomes and polymeric membranes have been prepared according to Scheme I: ring-opening copolymerization between 1,6-anhydro-2,4-di-*O*-benzyl-3-*O*-octadecyl- $\beta$ -D-glucopyranose (1) and 1,6-anhydro-2,3,4-tri-*O*-benzyl- $\beta$ -D-



glucopyranose (2) followed by debenzylation of the resulting copolymers. Polysaccharide synthesis via ring-opening polymerization of anhydro sugar derivatives is a useful method of preparing various polysaccharides of well-defined structures.<sup>16–18</sup> The required amount of long hydrocarbon chains could be introduced into (1→6)- $\alpha$ -D-glucopyranans regioselectively and at relatively uniform intervals. 3-*O*-Octadecyldextrans thus obtained are a biodegradable and hydrophilic–hydrophobic (amphiphilic)